ISSN 1063-7710, Acoustical Physics, 2014, Vol. 60, No. 2, pp. 223–234. © Pleiades Publishing, Ltd., 2014.

PHYSICAL FOUNDATIONS OF ENGINEERING ACOUSTICS

A Review on Sonic Crystal, Its Applications and Numerical Analysis Techniques[1]

Arpan Gupta

Department of Mechanical Engineering, Graphic Era University, Dehradun, Uttarakhand, 248002 India
e-mail: apn.gpt@gmail.com

Received May 4, 2013

Abstract—This paper presents a review study on sonic crystal, their development and present status. The paper also focuses on some of the applications of sonic crystal and numerical methods to study these crystals. Sonic crystals are periodic arrangement of scatterers, whose interaction with acoustic waves leads to the formation of band gap. Band gap are regions of frequencies where the sound propagation is significantly restricted from the sonic crystal. This property is used in many applications such as sound barrier, frequency filter, acoustic imaging etc. The paper presents a review of all these applications. Further the paper presents some of the numerical methods used to calculate the band gap formation in sonic crystal.

Keywords: sonic crystal, sound attenuation, sound barrier, frequency filter, acoustic imaging, numerical methods

DOI: 10.1134/S1063771014020080

Sonic crystals are artificial structures made by the periodic arrangement of scatterers in a square or triangular lattice configuration. The scatterers are sound hard (i.e., having a high acoustic impedance) with respect to the medium in which they are placed. For example, acrylic cylinders in air or steel plates in water are some examples of such sonic crystals. A sonic crystal with scatterers as cylinders arranged periodically is called a 2-D sonic crystal (Fig. 1). When the scatterers are placed in a 1-D periodic arrangement, such as steel plates placed periodically in water, it is known as a 1-D sonic crystal. When the scatterers such as spheres are placed in a 3-D periodic arrangement (for example, simple cubic), it is known as 3-D sonic crystal.

1. PERIODIC STRUCTURES AND BAND GAPS

Due to the periodic arrangement of scatterers, sonic crystals have a unique property of selective sound attenuation in specific range of frequencies. This range of frequencies is known as the band gap, and it is found that sound propagation is significantly reduced in this band gap region [1]. The reason for such sound attenuation is due to the destructive interference of waves in the band of frequencies. It is also shown numerically by author [2] that the propagating wave has an evanescent behavior (decaying amplitude) which causes the sound attenuation to take place in the band gap region.

Periodic structures, in general, can significantly alter the propagation of wave through them. The earliest realization of this principle was at the level of atomic structure in metals and semiconductors. According to quantum physics [3], atoms are arranged in a periodic lattice in a solid. When an electron (wave) passes through the crystal structure, it experiences a periodic variation in potential energy caused by the positive core of metal ions. The solution of Schrödinger equation over such a periodic arrangement is obtained by the Bloch theorem [3], or the Floquet theorem for 1-D case [4]. The wave propagating in such periodic structure is given as

$$\psi(r) = u(r)e^{ikr}, \quad (1)$$

where $\psi(r)$ is the Bloch function representing the electron wave function and $u(r)$ is a periodic function with periodicity of the lattice.

The solution of the Bloch wave for a periodic potential leads to the formation of bands of allowed and forbidden energy regions. The allowed energy regions are known as the conduction band and valence band, whereas the forbidden band of energies where there is no solution for the Bloch wave is known as the band gap. These band gaps are quite common in semiconductor materials and they form the basis of all modern electronic devices.

Another application of the same principle of wave interacting with periodic structures is in the field of photonic crystals [5, 6]. When an electromagnetic wave (light wave) passes through a periodic arrangement of dielectric material with different dielectric

[1] The article is published in the original.

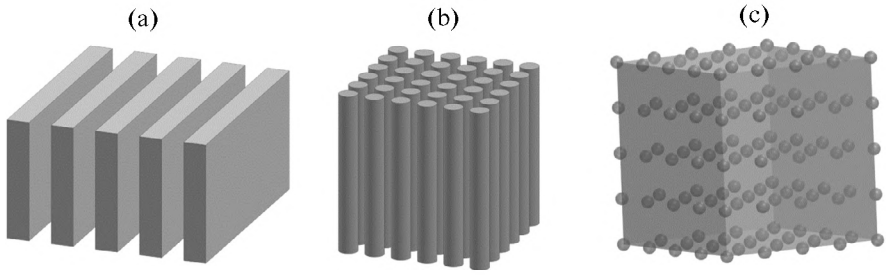

Fig. 1. Different types of sonic crystals. (a) 1-D sonic crystal consisting of plates arranged periodically; (b) 2-D sonic crystal with cylinders arranged on a square lattice; (c) 3-D sonic crystal consisting of periodic arrangement of sphere in simple cubic arrangement.

constants, photonic band gaps are formed. Therefore, there are certain frequencies of light that are allowed to pass through the structure and certain frequencies are restricted. The formation of band gaps allows the design of optical materials to control and manipulate the flow of light. One such practical application is the design of photonic crystal fiber [7], which uses microscale photonic crystals to confine and guide light.

The same principle is being extended and applied to the acoustic wave passing through the periodic structures. When an acoustic wave interacts with a periodic structure it forms bands of frequencies (Figs. 1, 2), where certain frequencies are allowed to pass through the structure without much attenuation, while certain frequencies are attenuated. This leads to significant sound attenuation in the frequency band. The band gap is represented by the shaded region in Fig. 2, where there is no solution of the frequency for a given wavenumber k. The band gap that extends for all directions of wave propagation is known as a complete band gap.

The present work is based upon assuming a planar wavefront for the propagating acoustic wave. However,

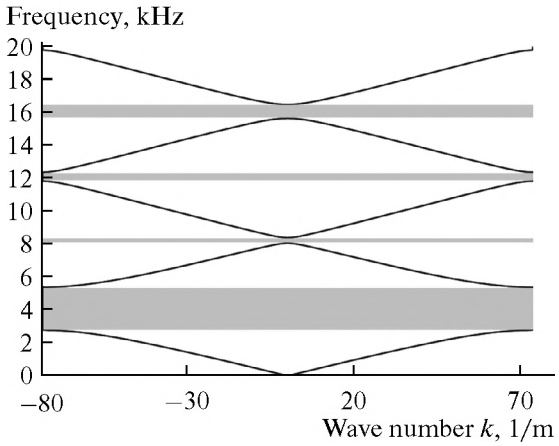

Fig. 2. An example of band gaps for a sonic crystal represented by the shaded region [2].

it is also shown that circular wavefront of wave can be considered [8] to give more accurate predictions.

One major difference between the periodic structure in the photonic crystal and in the sonic crystal is the size of the scatterers. For periodic structures to interact with waves, the scatterer dimension and the spacing between them should be of the order of wavelength of propagating wave [3]. In a photonic crystal the size of scatterers is of the order of microns [9], which is also the order of magnitude of the wavelength of electromagnetic wave. So a photonic crystal of the order of few millimeters has thousands of periodic units arranged in a periodic manner. An ideal or infinite periodic structure should have repeating units which extends till infinity. The band gap is actually obtained for an infinite structure. A photonic crystal having thousands of periodic units resembles an infinite periodic structure, and therefore in the band gap region there is no propagation of electromagnetic wave. For a sound wave in the audible region (20 Hz–20 kHz), the wavelength is of the order of few centimeters (1700–1.7 cm). Therefore, a sonic crystal due to practical considerations consists of few (3–10) scatterers arranged periodically and there is a significant sound attenuation in the band gap region. Authors have developed numerical methods [10] to obtain the band gap and also to obtain sound attenuation through a finite size of sonic crystal.

The first experimental measurement of sound attenuation by the sonic crystal was reported by Martinez-Sala et al. [1] in 1995. The sonic crystal was an artistic creation by Eusebio Sempere in Madrid consisting of a periodic array of steel cylinders as shown in Fig. 3. Experimental tests on this sculpture showed that there was a significant sound attenuation (~15 dB) at 1.67 kHz. This seminal work led to further investigation of acoustic waves passing over periodic structures. Such structures are called "Sonic crystals" (SC) or "Phononic crystals". Phononic crystals generally refer to structures made of similar host and scatterer material, such as nickel cylinders embedded in copper matrix etc., while sonic crystal refer to structure made of dissimilar materials, such as steel cylinders in water etc. Phononic crystal made of solid materials are for elastic wave propagation having both

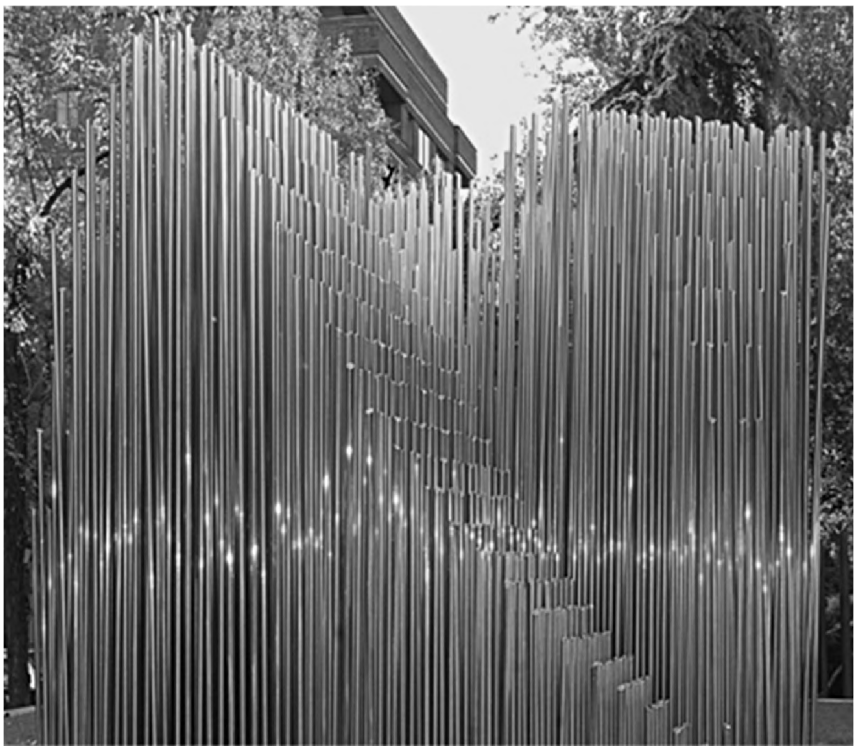

Fig. 3. First experimental revelation of the sonic crystal was found by an artistic structure designed by Eusebio Sempere in Madrid.

longitudinal and transverse wave components; while in the sonic crystal only longitudinal wave component is considered.

Sound propagation over a periodic arrangement of scatterers has been of interest over the past few decades. The first experimental observation of sound attenuation by a 2-D sonic crystal was made by Martinez et al. [1] in 1995, when it was found that an artistic creation has a possible engineering application. The structure was based on minimalistic design (an art movement in 1950's based on simplistic forms and designs), and consisted of hollow steel rods, 3 cm in outer diameter, arranged on a square lattice with a lattice constant of 10 cm. When sound propagates through this structure, it was found that certain bands of frequencies (centered around 1670 Hz) were significantly attenuated compared to other frequencies. The frequency corresponds to the destructive interference due to Bragg's reflection and thus the experimental measurements were explained by the opening up of first band gap in the periodic structure. This finding led to increased interest among researchers to explore sound propagation through periodic structures. Sigalas and Economou [11] obtained the band gap for the same experiment on the sculpture using the plane wave expansion method.

Dowling [12] has initially drawn correspondence from the electronic band gap in semiconductors and photonic band gap in photonic crystal and applied to sound wave. He has showed theoretically in 1992 that a one dimensional structure made by periodic variation in density of fluid will exhibit band gaps. James et al. [13] have demonstrated one dimensional sonic crystal made of perspex plates in water, theoretically and experimentally. They have also demonstrated that a narrow pass band can be obtained within the band gap by introducing a defect in the sonic crystal. Thus such structure can be used as a frequency filter.

2. SOUND INSULATION

Since the sound wave is inhibited to propagate through the sonic crystal in the band gap region, one of the direct applications of sonic crystal is in selective sound reduction. Multilayer partition based on periodic arrangement of layers showed the properties of one dimensional sonic crystal [14]. Such a one dimensional sonic crystal was able to overcome the increase in transmission at the critical frequency of the panel. Trees arranged in a two dimensional periodic arrangement [15] gave better sound attenuation compared to a green belt or forest. The frequencies attenuated corresponded to the periodicity of the lattice, and the array of trees works like a sonic crystal. Hence it was proposed that these periodic arrays of trees can be used as green acoustic screens. Similarly, in another study [16], periodic structures of size 1.11 m $\times$ 7.2 m with cylinders of diameter 16 cm were used as acoustic barriers in outdoors. The results showed good agreement with those predicted by Maekawa [17] for barriers.

Goffaux et al. [18] has also proposed using sonic crystals as an insulation partition. A comparison of sound attenuation by the sonic crystal inside the band gap is made with the mass law. It is shown that beyond nine periods of repeating unit, sonic crystal performs better than the mass law. There are similarly many experimental demonstration of sound attenuation in the band gap region [19–21]. Kushwaha [22] has proposed a multiperiodic tandem structure for obtaining a sound attenuation over a wide frequency range.

Batra et al. [23] has experimentally demonstrated three-dimensional sonic crystal made of lead spheres and brass beads in unsaturated polyester resin. The sound attenuation is explained on the basis of band gaps and it is proposed that such structures can be used for selective noise reduction.

Recently Krynkin et al. [24] has also studied the effect of a nearby surface on the acoustic performance of sonic crystal. They have validated their work with semi-analytical predictions based on multiple scattering theory and numerical simulations based on a boundary element formulations. It is concluded that the destructive interference of sound reflection by ground surface can significantly affect the transmission spectra.

The same author has also explained scattering by coupled resonating elements [25]. They have considered different types of resonators—empty N slip pipes and latex cylinder covered by a concentric PVC cylinder with four slits. It is shown that increase in slits causes an increase in frequency of Helmholtz resonator. Using such coupled resonators in sonic crystal can lead to low frequency sound attenuation.

Recently elastic shells with different material properties have also been used as the scattering element [26]. The resonance of such shells can improve in sound attenuation in the low frequency below the first band gap.

3. FREQUENCY FILTERS AND ACOUSTIC WAVEGUIDES

Sonic crystal can also be used as a frequency filter which does not allow sound wave to propagate in the band gap region. Another way of using sonic crystal as frequency filter is by introducing defects in the periodic structure. The defect mode corresponds to a narrow frequency pass band within the band gap. A one dimensional model of defect mode was presented by Munday et al. [27]. Khelif et al. demonstrated a tunable narrow pass band in a sonic crystal consisting of steel cylinders in water theoretically and experimentally [28, 29]. They have also shown that waveguides can be obtained by removing a single row of the scatterers [30, 31]. These waveguides are also demonstrated for tight bending of acoustic waves in the sonic crystal. Li et al. [32] has shown bending and branching of acoustic waves in V shape waveguides made from two-dimensional sonic crystal.

Pennec et al. [33] has theoretically investigated propagation of acoustic waves through the waveguides of steel hollow cylinders arranged periodically in water. They have demonstrated the presence of narrow pass band inside a broad stop band. The pass band can be adjusted by appropriately selecting the inner radius of the hollow cylinders or by filling the cylinders with a different density fluid. They have also extended this to a waveguide with hollow steel cylinders with two different inner radii varying alternatively. Such a novel waveguide has been shown to have two narrow pass bands corresponding to individual radii of hollow cylinder. An active guiding device is proposed by changing the fluid in these two different cylinders. Also, a Y-shaped waveguide is shown to act as a multiplexer and demultiplexer for separating and merging signals with different frequencies.

Miyashita et al. [34, 35] has demonstrated experimentally sonic crystal waveguide made by acrylic cylinders in air. Straight waveguide and sharp bending waveguide composed of line of single defect are shown to have a good transmission in a narrow pass band. They have proposed waveguides based on defect in sonic crystal as potential application in acoustic circuits made on sonic crystal slab.

4. METAMATERIALS AND RADIAL WAVE CRYSTAL

Recently, there has been an immense growth in the area of metamaterials, due to their ability to manipulate light and sound waves, which are not available in nature. Metamaterials are artificial structures made by periodic arrangement of scatterers, similar to sonic crystal, but in this case the periodic units are much smaller than the wavelength propagating over the structure. As a result, the wave sees an "effective material properties." It is something like replacing natural atoms by larger man-made atoms. The result of such design leads to unique material properties such as negative density, negative bulk modulus, negative refractive index, etc.

The first concept of metamaterial was proposed by Veselago for the electromagnetic wave in 1968 [36]. Later on Pendry et al. [37, 38] proposed artificial structure materials having effective negative permeability and permittivity. The negative refractive index material was first demonstrated at GHz frequency [39, 40].

The first experimental evidence of acoustic metamaterial was observed by Liu et al. [41], where locally resonant sonic materials demonstrated negative effective dynamic density. Recently, Fang et al. [42] has also proposed acoustic metamaterial based on Helmholtz resonators which exhibit negative effective modulus. The feasibility of such negative effective material properties has led to very interesting applications. One such application is in cloaking, or making

an object invisible to electromagnetic [43, 44] or acoustic wave [45–48].

Torrent et al. [49, 50] has also recently proposed a new kind of metamaterial known as radial wave crystal which are metamaterials in polar or radial coordinate. They have demonstrated that such metamaterials possess anisotropic material properties. The material properties of density tensor and bulk modulus were obtained from the property of invariable in translation on the governing wave equation from one unit cell to another. We have used similar concept to design a radial sonic crystal to attenuate sound propagating with circular wavefront.

Arc shared phononic crystal have also been studied recently using transfer matrix method in cylindrical coordinates [51].

5. OTHER APPLICATIONS

Another interesting application of sonic crystals is in sound diffusers [52] in room. Such diffusers can help in improving the acoustic performance of a room by reducing the echo and increasing the sound field diffusiveness, especially at low frequencies.

Sonic crystals have also been shown for the application of acoustic diode for unidirectional sound propagation [53]. Previously it has been demonstrated that it requires strongly nonlinear materials to break the time reversal symmetry in a structure [54, 55]. However, in this recent work Li et al. [53] have experimentally realized unidirectional sound transmission through the sonic crystal. The nonreciprocal sound transmission is controlled simply by mechanically rotating the square cylinders of the sonic crystal. Li et al. [53] also claims that the new model of sonic crystal based acoustic diode being a linear system is more energy efficient and operates at a broader bandwidth than the acoustic rectification based on nonlinear materials.

Sonic crystal is also used for an application of liquid sensor [56]. The liquid sensor is designed based on the transmission spectra of the sonic crystal. The shift in the band gap is used to predict the material properties of the liquid. Sonic crystal is also used to exhibit the phenomenon of resonant tunneling [57, 58].

6. NUMERICAL METHODS FOR CALCULATION AND OPTIMIZATION OF THE BAND GAP

All the applications of the sonic crystal are primarily based on the prediction of the band gap. The band gap is characterized by the position (center frequency) and the width of the band gap. There are methods such as plane wave expansion method [11, 59–61] and multiple scattering method [62, 63] for calculating the band structure. These methods were mainly developed for photonic and phononic crystals which were also extended to sonic crystal.

The first complete band gap calculation for periodic elastic composites was presented by Kushwaha et al. in 1993 [64]. The computation was performed for nickel alloy cylinders in aluminum alloy background and vice versa. Phononic band gaps have also been obtained using a 1-D and 2-D periodic spring mass system by Jensen [65]. Acoustic band gaps have also been shown for silica cylinders in viscous liquid [66]. Plane wave expansion method is used to investigate the effect of viscosity and it has been shown that viscosity can lead to larger band gaps. Band gaps are also shown for time varying materials [67]. Thus by varying the material properties of the phononic crystal, band gaps can be modified dynamically. Band gaps have also been optimized using structure topology optimization [68]. Band gaps can also be tuned by placing additional rods in the unit cell [69].

Miyashita [70] has demonstrated experimentally sound attenuation by an array of 10×10 acrylic cylinders. He has explained the sound reduction by obtaining sound transmission over a finite periodic structure using the finite difference time domain method. However, this method is computationally expensive, as one solves the wave propagation over two dimensional periodic structures in real time. The space discretization is restricted by the wavelength of propagating wave and the time step is restricted by the Courant's condition, which makes this method computationally very expensive. In another similar work [59], they have used 10×10 copper cylinders in air. Sound transmission through the sonic crystal was obtained experimentally, which was compared with the numerical prediction from the finite difference time domain method and band gap calculation from the plane wave expansion method. It was further shown that since the impedance mismatch between copper and air is very high, sound transmission through the hollow and filled cylinders is the same. Therefore, the cylinders boundary can be effectively modeled as sound hard boundaries.

An improved numerical method based on finite difference time domain method was proposed by Cao et al. [71] to obtain the band structure. The method is shown to overcome the convergence problem of the plane wave expansion method for liquid cylinder in solid matrix. The computational time is also reduced compared to the conventional finite difference time domain method.

Chen and Ye [72] have shown that as the cylinders are randomized, the sound attenuation is improved over a wide range of frequencies. Band gap have also been shown to increase by reducing the symmetry of the structure [73]. Goffaux [74] has also shown that the band gaps can be tuned or controlled by rotating the sonic crystal made of rectangular scatterers. Tunable acoustic band gap are also shown for sonic crystal made of dielectric elastomer cylindrical actuator [75]. Applying voltage to the dielectric elastomer cylindrical

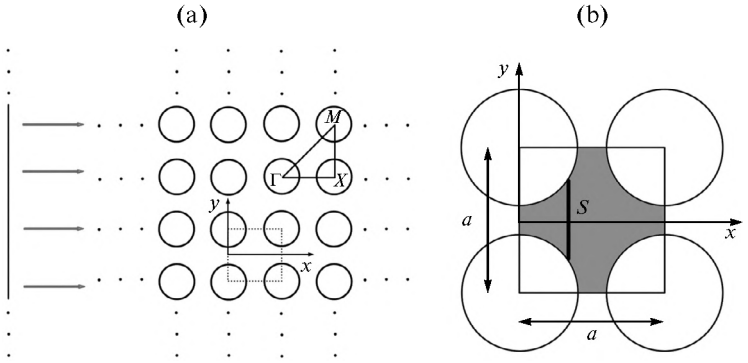

Fig. 4. (a) A two dimensional periodic structure made of circular scatterers arranged on a square lattice. On the left side there is plane wave sound source. The dotted square shows a unit cell. (b) Magnified view of a unit cell with various geometric parameters.

actuator causes a radial strain in the cylinders which affects the band gap.

Kushwaha [76] has also studied a three dimensional sonic crystal made of air bubbles in water in different configurations such as, face-centered cubic, body-centered cubic and simple-cubic. Such structure with huge difference in acoustic impedance has been reported to have widest band gap [77]. Kushwaha et al. [78] has performed band gap calculations for three dimensional sonic crystal made of rigid spheres and cubes in air. They have also proposed a tandem structure that allows for an ultrawideband filter for environmental or industrial noise in the desired frequency range. Band gap calculated for cubical array of hydrogen spheres in air [79].

7. EVANESCENT WAVE

Recently, an extended plane wave expansion (EPWE) method has been proposed [80, 81] to compute the complex band structure [82] of the sonic crystal. The complex band structure gives the additional information of the decay constant (imaginary part of wavenumber) of the sound wave in the band gap region. Also, it has been shown that for a finite structure or for structures having defects, the propagating wave is evanescent in nature [83]. Therefore, using the decay constant, sound attenuation through the finite arrangement of scatterers can be obtained.

The complex band gap is important because we rarely find an "infinite" sonic crystal, especially for applications of sound wave in audible frequency range. The dimension of sonic crystal (based on Bragg's reflection) depends on the wavelength of the sound wave, which is quite large (~few cm) for the audible frequency range. Therefore, the sonic crystal has a finite number of scatterers and it is important to evaluate the performance of a finite sonic crystal. There are methods such as finite difference time domain method to obtain transmission coefficient through the finite sonic crystal, but such methods are computationally very expensive. However, obtaining the attenuation through the decay constant gives a quick check on the sound attenuation level expected by the structure in the band gap region.

8. NUMERICAL METHOD

In the present section, numerical method developed by author [2, 10, 84–86] is presented. Sound propagation over a two dimensional sonic crystal is considered. The scatterers are sound hard cylinders with diameter 3 cm, arranged on a square lattice with lattice constant of 4.25 cm. The sonic crystal is shown in Fig. 4a. The sound wave with a planar wavefront propagates along the symmetry direction (ΓX) of the periodic structure. The triangle ΓX represents the irreducible part of the first Brillouin zone [3]. Because of the symmetry, wave propagation in any direction can be represented by wave propagation along the irreducible part of the Brillouin zone. However, in the present study, sound propagation is considered only along the symmetric direction ΓX.

The periodic structure is represented by a unit cell as shown by the dotted square in Fig. 4a. Simple translation of this unit cell can form the whole periodic structure. Figure 4b shows the magnified view of the unit cell with some geometric parameters. The lattice constant is given by a which is the center to center distance between the adjacent scatterers. Since this is a square lattice, therefore the lattice constant is the same in both x and y directions.

Sound propagation through the unit cell takes place through the air (shaded region in Fig. 4b) as the scatterers are sound hard with respect to air. Sound propagation can thus be modeled by the Webster horn equation [87, 88]

$$\frac{d^2p(x,t)}{dt^2} = \frac{c^2}{S}\frac{d}{dx}\left(S\frac{dp(x,t)}{dx}\right), \qquad (2)$$

where p is the pressure, c is the velocity of sound in air and S is the variable cross sectional area. The cross sectional area S is perpendicular to the direction of wave propagation and is represented by the vertical

bold line in Fig. 4b. Furthermore, we consider the case when pressure is harmonic, and the signal can be represented as a sum of harmonic functions

$$p(x, t) = \mathrm{Re}(P(x)e^{i\omega t}), \quad (3)$$

where $P(x)$ is a complex-valued amplitude.

For a harmonic response, the Webster horn equation further reduces to Eq. (4):

$$\frac{d^2P}{dx^2} + \frac{dP}{dx}\left(\frac{S'}{S}\right) + \frac{\omega^2}{c^2}P = 0, \quad (4)$$

where S' represents the first derivative of S with respect to x and ω is the angular frequency of the propagating wave.

Wave propagation in a periodic structure, as shown by Fig. 4a, can be restricted to a unit cell (Fig. 4b) by using the Bloch theorem [3] or the Floquet theorem for 1-D case [4]. The wave propagating in such a periodic structure is given as

$$p(x) = e^{ikx}\varphi(x), \quad (5)$$

where $\varphi(x)$ is a periodic function with periodicity a, i.e. $\varphi(a + x) = \varphi(x)$. Bloch waves are plane waves (e^{ikx}) modulated with a periodic function $\varphi(x)$, which has the same periodicity as that of the lattice structure.

Using the Floquet theorem with the Webster horn equation in a unit cell, the governing equation reduces to the following equation:

$$\left\{\frac{d^2\varphi}{dx^2} + \frac{d\varphi}{dx}\left(2ik + \frac{S'}{S}\right) + \varphi\left(ik\frac{S'}{S} - k^2\right)\right\} + \frac{\omega^2}{c^2}\varphi = 0. \quad (6)$$

The above equation is solved using the finite difference method. The unit cell is divided into N segments of length h with $(N + 1)$ points in the x direction. A second order central difference scheme is used for the finite difference discretization:

$$\frac{d^2\varphi}{dx^2} = \left(\frac{\varphi_{j+1} - 2\varphi_j + \varphi_{j-1}}{h^2}\right) + O(h^2), \quad (7)$$

$$\frac{d\varphi}{dx} = \left(\frac{\varphi_{j+1} - \varphi_{j-1}}{2h}\right) + O(h^2). \quad (8)$$

As the structure is periodic, periodic boundary conditions are applied at the first and last node of the discretized geometry.

This transforms Eq. (6) to an eigenvalue problem given by Eq. (9).

$$[A(k)]\{\varphi\} + \frac{\omega^2}{c^2}\{\varphi\} = 0, \quad (9)$$

where A is a matrix whose coefficients are function of the wavenumber k which is varied in the first Brillouin zone $\left(-\frac{\pi}{a} \le k \le \frac{\pi}{a}\right)$. The solution to the eigenvalue problem (Eq. (9)) results in the feasible values of frequencies that can propagate through the structure. This results in the band structure or the dispersion relation for periodic structure as shown in Fig. 5. The band structure is a plot between the frequency and wavenumber. The band gaps are represented by the shaded region where there is no real wave that can propagate through the periodic structure.

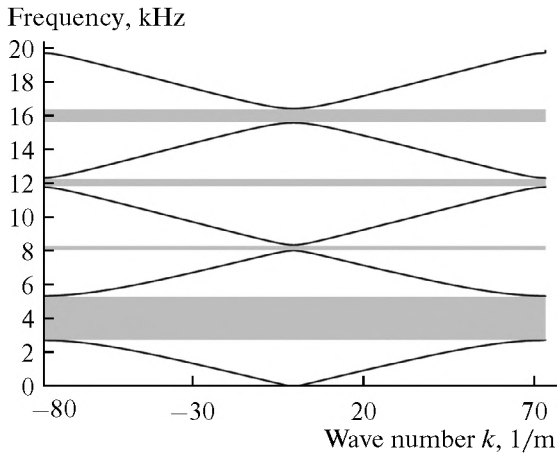

Fig. 5. Band gap for an infinite sonic crystal corresponding to Fig. 3.1 with $a = 4.25$ cm and $d = 3$ cm, along the symmetry direction ΓX.

The band gap calculation shows that the first band gap opens up at a frequency band of 2795–5470 Hz. A band gap is represented by two parameters: center frequency and band width. The center frequency of the band gap is the mean frequency of the band gap, which in this case is 4132 Hz. The center frequency of the periodic structure can also be predicted by the Bragg's law [89] given by Eq. (10):

$$f_c = \frac{c}{2a}. \quad (10)$$

The center frequency from the Bragg's law prediction is 4035 Hz, which is quite close to the center frequency predicted by the numerical model (4132 Hz).

Another representative parameter of a band gap is the band width which is the difference between the upper and lower frequencies of a band gap. The band width for the first band gap is 2675 Hz.

In the band gap region of 2795–5470 Hz, no propagating wave exist for an "infinite sonic crystal." There are other band gaps at higher frequencies, three of which are shown by the shaded region in Fig. 5. However, the band widths of the three band gaps are quite small.

9. COMPLEX FREQUENCY BAND STRUCTURE AND DECAY CONSTANT

In the last section, a method to obtain band gaps is described where there is no solution to the wave fre-

quency for a given wavenumber varying in the first Brillouin zone. As mentioned in previously, there are many other methods to obtain band gap. However, band gap does not give any information about the sound attenuation over the finite sonic crystal.

In this section, a method is presented to obtain decay constant and complex band gap which can predict sound attenuation by the sonic crystal in the band gap region. Decay constant is the imaginary part of the wavenumber, which predicts evanescent wave in the band gap region. The attenuation in the evanescent wave over a finite length can be obtained numerically, which gives the sound attenuation by the finite sonic crystal. The combined plot of band gap along with the decay constant is referred as the complex band gap or complex dispersion relation.

In the previous section, it was shown that Webster horn equation along with Floquet theorem leads to a differential equation given by Eq. (6), which reduces to an eigenvalue problem (Eq. (9)) using the finite difference discretization and periodic boundary condition. For this case, the independent variable was wavenumber k and the problem was solved for feasible values of angular frequency ω. Equation (6) can be reformulated in the reverse way with the independent variable being angular frequency, and solving for the dependent variable wavenumber:

$$k^2\{-\varphi\} + k\left\{2i\frac{d\varphi}{dx} + \varphi\left(i\frac{S'}{S}\right)\right\} + \left\{\frac{d^2\varphi}{sx^2} + \frac{d\varphi}{dx}\left(\frac{S'}{S}\right) + \frac{\omega^2}{c^2}\varphi\right\} = 0. \quad (11)$$

The above equation when discretized using finite difference equations (Eqs. (7), (8)) along with periodic boundary condition leads to the following quadratic eigenvalue problem in wavenumber:

$$[A_2]\{\varphi\}k^2 + [A_1]\{\varphi\}k + [A_0]\{\varphi\} = 0, \quad (12)$$

where, A_i are all matrices of size $N \times N$, with known coefficients which are function of frequency and $\{\varphi\}$ is the eigenvector of size $N \times 1$. The matrices A_0 and A_1 are periodic tridiagonal matrices, whose coefficients are given as

$$(A_0)_{m,m-1} = \frac{1}{h^2} - \frac{S'}{2Sh}, \quad (A_0)_{m,m} = \left(\frac{\omega}{c}\right)^2 - \frac{2}{h^2},$$

$$(A_0)_{m,m+1} = \frac{1}{h^2} + \frac{S'}{2Sh} \text{ for } 2 \le m \le N-1.$$

Due to the periodicity of the unit cell, the first and last rows are given by

$$(A_0)_{1,1} = \left(\frac{\omega}{c}\right)^2 - \frac{2}{h^2}, \quad (A_0)_{1,2} = \frac{1}{h^2} + \frac{S'}{2Sh},$$

$$(A_0)_{1,N} = \frac{1}{h^2} - \frac{S'}{2Sh}, \quad (A_0)_{N,1} = \frac{1}{h^2} + \frac{S'}{2Sh},$$

$$(A_0)_{N,N-1} = \frac{1}{h^2} - \frac{S'}{2Sh}, \quad (A_0)_{N,N} = \left(\frac{\omega}{c}\right)^2 - \frac{2}{h^2}.$$

Similarly coefficients of periodic tridiagonal matrix A_1 are

$$(A_1)_{m,m-1} = -\frac{i}{h}, \quad (A_1)_{m,m} = i\frac{S'}{S}, \quad (A_1)_{m,m+1} = \frac{i}{h}$$

for $2 \le m \le N-1$. $(A_1)_{1,1} = i\frac{S'}{S}$, $(A_1)_{1,2} = \frac{i}{h}$,

$$(A_1)_{1,N} = -\frac{i}{h}, \quad (A_1)_{N,1} = \frac{i}{h} \quad (A_1)_{N,N-1} = -\frac{i}{h},$$

$$(A_1)_{N,N} = i\frac{S'}{S}.$$

Lastly, A_2 is a diagonal matrix with diagonal element as

$$(A_2)_{m,m} = -1 \text{ for } 1 \le m \le N.$$

The above quadratic eigenvalue problem (Eq. (12)) is solved by rearranging the equation in a linear form as shown below:

$$\begin{pmatrix} -A_0 & 0 \\ 0 & I \end{pmatrix}\begin{Bmatrix} \phi \\ k\phi \end{Bmatrix} = \begin{pmatrix} A_1 & A_2 \\ I & 0 \end{pmatrix}\begin{Bmatrix} \phi \\ k\phi \end{Bmatrix}, \quad (13)$$

which is solved using a standard eigenvalue solver in Matlab to obtain k. In general, the wavenumber k for a given frequency is found to be a complex number:

$$k = k_R + ik_I, \quad (14)$$

where k_R and k_I are the real and imaginary parts, respectively.

In a unit cell, the pressure variation is given by Eq. (5). The complex wavenumber $k = k_R + ik_I$ causes as exponential decay in the amplitude of wave due to the imaginary part of the wavenumber k_I:

$$P(x) = \varphi(x)\exp(-k_I x)\exp(ik_R x). \quad (15)$$

If k is real valued ($k_I = 0$), wave propagates with constant amplitude. For a positive imaginary part ($k_I > 0$), wave has an evanescent behavior, leading to attenuation in the amplitude of pressure wave in the propagating direction. The value of k_I gives us the decay in the amplitude of the wave, and hence it is referred as the decay constant. The decay constant and complex band structure is plotted in Fig. 6. The first band gap predicted is from 2795–5470 Hz with the center frequency of 4132 Hz. The maximum value of decay constant at the center frequency is found to be 24.75.

As it can be seen from the figure, the band gap corresponds to the range of frequencies where a nonzero value of k_I exists. Thus, for a finite sonic crystal, the

propagating wave undergoes sound attenuation for the frequencies corresponding to the band gap. Based on Eq. (15), sound attenuation (in dB) over a length x is calculated as

$$Attenuation = 20 \times \log(1/\exp(-k_I x)). \quad (16)$$

The sound attenuation over a length of five unit cells (0.21 m) is predicted by the decay constant and is plotted in Fig. 7 for a frequency range of 500–6000 Hz. The sound attenuation in the band gap region is not uniform; rather it is elliptic in nature. The maximum sound attenuation is found to be 45 dB at the center frequency of the band gap.

10. SOUND ATTENUATION BY THE SONIC CRYSTAL USING THE WEBSTER HORN EQUATION

Sound attenuation by a finite sonic crystal can be directly obtained by modeling the sonic crystal as a waveguide and obtaining sound transmission through the waveguide using the Webster horn equation. The difference between previous sections and this section is that no periodic condition, such as Bloch theorem or Floquet theorem, is implemented in the formulation. The periodicity is in the geometry of the waveguide.

The problem considered is shown in Fig. 8a with sonic crystal consisting of five layers of scatterers. A planar sound wave propagates along the symmetry direction (ΓX) of the sonic crystal. Since the problem is symmetric about AB and CD, the model can be reduced to a strip model as shown by the rectangle in Fig. 8a.

The model is further reduced by taking the symmetry about the center line to give a waveguide as shown in Fig. 8b. The top and bottom surfaces including the cylinders are modeled as sound hard boundaries. There is a sound source at the inlet end, and radiation boundary condition is applied at the outlet end. The problem is effectively reduced to one of sound propagation through a symmetric waveguide as shown in Fig. 8b which is solved using the Webster horn equation.

Sound propagating through a waveguide with a variable cross-sectional area is modeled by the Webster horn equation. The Webster horn equation considers pressure to be a function of the direction of wave propagation, and constant over the cross-section of the waveguide. This reduces the problem to a 1-D model represented by an ordinary differential equation. For harmonic excitation, the Webster horn equation is given by the Eq. (4), where S is represented by the cross-sectional area of the waveguide as shown in Fig. 8b.

The Webster horn equation is discretized along the x-axis using the second-order finite difference method to obtain a system of linear equations. The radius of cylinders r is 1.5 cm and lattice spacing a is 4.25 cm.

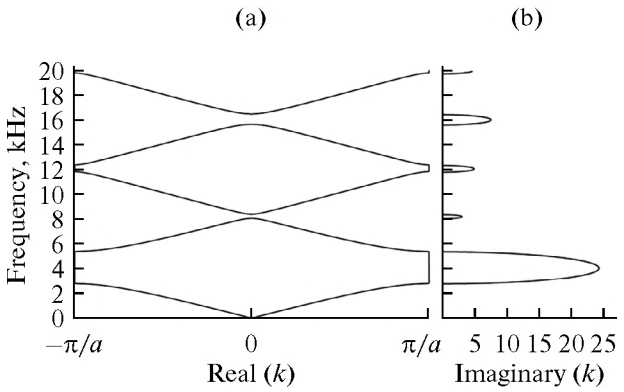

Fig. 6. Complex band structure for an infinite sonic crystal. (a) Normal band structure. (b) Decay constant as a function of frequency. The decay constant is non-zero in the band gap regions.

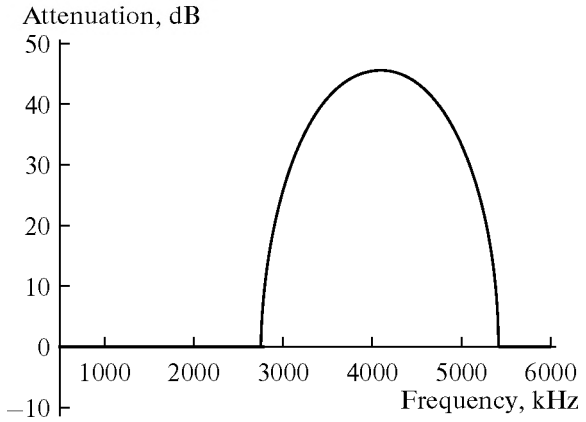

Fig. 7. Sound attenuation predicted by the decay constant.

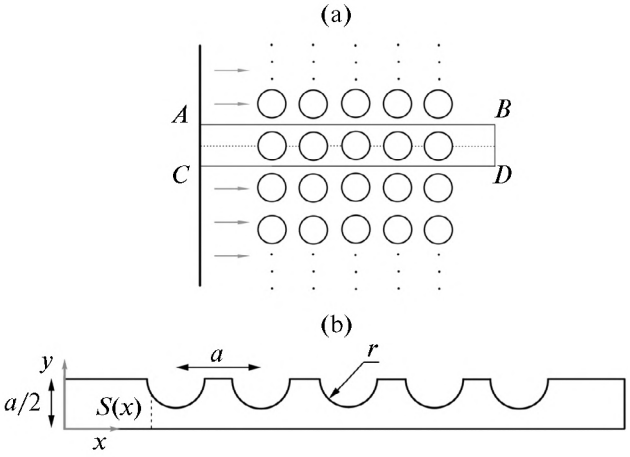

Fig. 8. (a) Sound propagating over a sonic crystal consisting of five layers of scatterers. Using symmetry of the structure, the problem is reduced to a strip model shown by rectangle ACDB. (b) A symmetric waveguide used to model sound propagation through the sonic crystal using Webster horn equation.

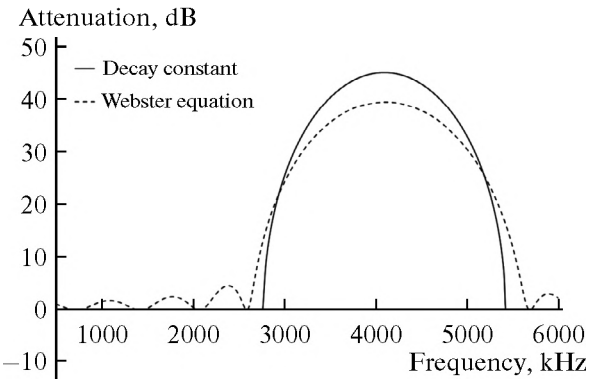

Fig. 9. Sound attenuation by the finite sonic crystal using the Webster horn equation and decay constant.

The cross-sectional area function $S(x)$ is shown in Fig. 8b by the dashed line. The numerical results for pressure were found to converge for 2000 mesh points, for frequency up to 6000 Hz.

Sound attenuation by the sonic crystal is given by the insertion loss.

$$IL = SPL_{without\,SC} - SPL_{with\,SC}, \tag{17}$$

where $SPL_{without\,SC}$ and $SPL_{with\,SC}$ are the sound pressure levels at the same position without and with the sonic crystal, respectively. Sound pressure is obtained 10 cm (~2.5a) away from the last cylinder. The pressure amplitude obtained at this position corresponds to sound pressure level with the sonic crystal ($SPL_{with\,SC}$). When the cylinders are removed, the waveguide becomes a straight channel with uniform pressure amplitude across the cross-section, as the other end has the radiation boundary condition. Therefore, the sound pressure level without cylinders at the same position is the same as that corresponding to the incident wave amplitude when the cylinders are present.

Using the standard definition of sound pressure level, the above expression for insertion loss reduces to

$$IL = 20 \times \log_{10}\left(\frac{P_I}{P_O}\right), \tag{18}$$

where P_I is the amplitude of the inlet pressure wave that is incident on the sonic crystal and P_O is the amplitude of the outgoing pressure wave measured 10 cm after the last cylinder.

At the inlet boundary, a sound source with pressure of 1 Pa was prescribed. However, the prescribed pressure at the inlet boundary is not the forward traveling incident wave. The pressure at the inlet boundary is the resultant of forward traveling incident wave and backward traveling reflected wave. Pressure and velocity condition at the inlet boundary are used to extract the incident pressure wave.

The net pressure at the inlet can be written as a combination of forward and backward travelling wave:

$$\begin{aligned} p(x,t) &= \mathrm{Re}\{P_I e^{i(\omega t - kx)} + P_R e^{i(\omega t + kx)}\} \\ &= \mathrm{Re}\{P(x)e^{i\omega t}\}, \end{aligned} \tag{19}$$

therefore,

$$P(x) = P_I e^{-ikx} + P_R e^{ikx}, \tag{20}$$

where P_I and P_R are the amplitudes of the incident and reflected wave, respectively.

Similarly, the velocity is given as [88]

$$\begin{aligned} u(x,t) &= \mathrm{Re}\left\{\frac{1}{\rho c}(P_I e^{i(\omega t - kx)} - P_R e^{i(\omega t + kx)})\right\} \\ &= \mathrm{Re}\{U(x)e^{i\omega t}\}, \end{aligned} \tag{21}$$

where

$$U(x) = \frac{1}{\rho c}(P_I e^{-ikx} - P_R e^{ikx}). \tag{22}$$

At the inlet ($x = 0$), Eqs. 20 and 3.22 reduces to

$$P|_{x=0} = P_I + P_R, \tag{23}$$

$$U|_{x=0} = \frac{P_I}{\rho c} - \frac{P_R}{\rho c}. \tag{24}$$

The above set of simultaneous equations is solved to get the amplitude of incident forward traveling wave as a function of inlet boundary pressure P and velocity U at the boundary:

$$P_I = \left(\frac{P + \rho c U}{2}\right)\Bigg|_{x=0}. \tag{25}$$

The outgoing wave amplitude (P_O) can be directly obtained from the pressure field in the output region as there is no reflected wave in the output region.

In this way, sound attenuation at a particular frequency is obtained. The procedure is repeated for a range of frequencies from 500 to 6000 Hz with a frequency step of 10 Hz, to obtain the sound attenuation by five cylindrical scatterers arranged periodically. Sound attenuation by the finite sonic crystal using the Webster horn equation and from the decay constant is plotted in Fig. 9.

The sound attenuation by the Webster horn equation for a finite sonic crystal shows significant sound attenuation (>20 dB) in the band gap region—2795–5470 Hz, as predicted by the 1-D model. Further the sound attenuation magnitude is quite close to the predictions made by the decay constant. Decay constant is based on an infinite sonic crystal, therefore, for the frequencies not in the band gap (such as below 2500 Hz), sound attenuation is zero. However, for a finite sonic crystal, there is a finite sound attenuation, which increases significantly in the band gap region.

11. CONCLUSIONS

The paper presents some of the recent findings related to sonic crystal. The paper discusses the basis of sonic crystal to provide a band gap or frequency

range where there is high sound attenuation. The paper discusses some of the applications of sonic crystal in sound insulation, frequency filter, acoustic waveguides, metamaterials, radial wave crystal, etc. The paper also discusses about some of the numerical methods used for the calculation and prediction of band gap. Sonic crystal thus provides a very interesting way to control and manipulate the sound wave.

REFERENCES

1. J. Martinez-Sala, J. V. Sancho, V. Sanchez, J. Gomez, J. Llinarez, and F. Meseguer, Nature **378**, 241, (1995).
2. A. Gupta, K. M. Lim, and C. H. Chew, Appl. Phys. Lett. **98**, 201906 (2011).
3. C. Kittel, Introduction to Solid State Physics (Wiley, New York, 2005, 8th ed.; Nauka, Moscow, 1978).
4. J. Mathews and R. L. *Walker, Mathematical Methods of Physics*. 2nd ed. (Benjamin, California, 1969).
5. E. Yablonovitch, Phys. Rev. Lett. **58**, 2059 (1987).
6. S. John, Phys. Rev. Lett. **58**, 2486 (1987).
7. P. Russell, Science **299**, 358 (2003).
8. A. Gupta, K. M. Lim, and C. H. Chew, Acoust. Phys. **59**, 493 (2013).
9. J. D. Joannopoulos, P. R. Villeneuve, and S. H. Fan, Nature **386**, 143 (1997).
10. A. Gupta, K. Lim, and C. Chew, J. Acoust. Soc. Am. **132**, 2909 (2012).
11. M. M. Sigalas and E. N. Economou, Europhys. Lett. **36**, 241 (1996).
12. J. P. Dowling, J. Acoust. Soc. Am. **91**, 2539 (1992).
13. R. James, S. M. Woodley, C. M. Dyer, and V. F. Humphrey, J. Acoust. Soc. Am. **97**, 2041 (1995).
14. A. Uris, C. Rubio, H. Estelles, J. V. Sanchez-Perez, R. Martinez-Sala, and J. Llinares, Appl. Phys. Lett. **79**, 4453 (2001).
15. R. Martinez-Sala, C. Rubio, L. M. Garcia-Raffi, J. V. Sanchez-Perez, E. A. Sanchez-Perez, and J. Llinares, J. Sound Vibr. **291**, 100 (2006).
16. J. V. Sanchez-Perez, C. Rubio, R. Martinez-Sala, R. Sanchez-Grandia, and V. Gomez, Appl. Phys. Lett. **81**, 5240 (2002).
17. Z. Maekawa, Appl. Acoust. **1**, 157 (1968).
18. C. Goffaux, F. Maseri, J. O. Vasseur, B. Djafari-Rouhani, and P. Lambin, Appl. Phys. Lett. **83**, 281 (2003).
19. C. Rubio, D. Caballero, J. V. Sanchez-Perez, R. Martinez-Sala, J. Sanchez-Dehesa, F. Meseguer, and F. Cervera, J. Lightwave Technol. **17**, 2202 (1999).
20. M. S. Kushwaha and B. Djafari-Rouhani, J. Sound Vibr. **218**, 697 (1998).
21. J. V. Sanchez-Perez, D. Caballero, R. Martinez-Sala, C. Rubio, J. Sanchez-Dehesa, F. Meseguer, J. Llinares, and F. Galvez, Phys. Rev. Lett. **80**, 5325 (1998).
22. M. S. Kushwaha, Appl. Phys. Lett. **70**, 3218 (1997).
23. N. K. Batra, P. Matic, and R. K. Everett, in *Proc. Ultrasonics Symp., 2002* (Proc. IEEE, Vol. 1), 2002.
24. A. Krynkin, O. Umnova, J. V. Sanchez-Perez, A. Yung Boon Chong, S. Taherzadeh, and K. Attenborough, J. Acoust. Soc. Am. **130**, 3736 (2011).
25. A. Krynkin, O. Umnova, A. Y. B. Chong, S. Taherzadeh, and K. Attenborough, J. Phys. D: Appl. Phys. **44**, 125501 (2011).
26. A. Krynkin, O. Umnova, A. Y. B. Chong, S. Taherzadeh, and K. Attenborough, J. Acoust. Soc. Am. **128**, 3496 (2010).
27. J. N. Munday, C. B. Bennett, and W. M. Robertson, J. Acoust. Soc. Am. **112**, 1353 (2002).
28. A. Khelif, P. A. Deymier, B. Djafari-Rouhani, J. O. Vasseur, and L. Dobrzynski, J. Appl. Phys. **94**, 1308 (2003).
29. A. Khelif, A. Choujaa, B. Djafari-Rouhani, M. Wilm, S. Ballandras, and V. Laude, Phys. Rev. B: Condens. Matter Mater. Phys. **68**, 214301 (2003).
30. A. Khelif, A. Choujaa, S. Benchabane, B. Djafari-Rouhani, and V. Laude, Appl. Phys. Lett. **84**, 4400 (2004).
31. A. Khelif, A. Choujaa, S. Benchabane, V. Laude, and B. Djafari-Rouhani, in *Proc. IEEE Ultrasonics Symp., 2004*.
32. X. Li and Z. Liu, Phys. Lett. A: Gener., At. Solid State Phys. **338**, 413 (2005).
33. Y. Pennec, B. Djafari-Rouhani, J. O. Vasseur, A. Khelif, and P. A. Deymier, Phys. Rev. E: Statist., Nonlin., Soft Matter Phys. **69**, 046608 (2004).
34. T. Miyashita, Measur. Sci. Technol. **16**, R47 (2005).
35. T. Miyashita, Jap. J. Appl. Phys. Part 1: Regular Papers Brief Commun. Rev. Papers **45**, 4440 (2006).
36. V. G. Veselago, Sov. Phys. Usp. **10**, 509 (1968).
37. J. B. Pendry, A. J. Holden, D. J. Robbins, and W. J. Stewart, IEEE Trans. Microwave Theory Tech. **47**, 2075 (1999).
38. J. B. Pendry, A. J. Holden, W. J. Stewart, and I. Youngs, Phys. Rev. Lett. **76**, 4773 (1996).
39. D. R. Smith, W. J. Padilla, D. C. Vier, S. C. Nemat-Nasser, and S. Schultz, Phys. Rev. Lett. **84**, 4184 (2000).
40. R. A. Shelby, D. R. Smith, and S. Schultz, Science **292**, 77 (2001).
41. L. Zhengyou, Z. Xixiang, M. Yiwei, Y. Y. Zhu, Y. Zhiyu, C. T. Chan, and S. Ping, Science **289**, 1734 (2000).
42. N. Fang, D. J. Xi, J. Y. Xu, M. Ambati, W. Srituravanich, C. Sun, and X. Zhang, Nature Mater. **5**, 452 (2006).
43. J. B. Pendry, D. Schurig, and D. R. Smith, Science **312**, 1780 (2006).
44. D. Schurig, J. J. Mock, B. J. Justice, S. A. Cummer, J. B. Pendry, A. F. Starr, and D. R. Smith, Science **314**, 977 (2006).
45. H. Y. Chen and C. T. Chan, Appl. Phys. Lett. **90**, 241105 (2007).
46. D. Torrent and J. Sanchez-Dehesa, New J. Phys. **10**, 063015 (2008).
47. S. A. Cummer and D. Schurig, New J. Phys. **9**, 45 (2007).
48. S. Zhang, C. G. Xia, and N. Fang, Phys. Rev. Lett. **106**, 024301 (2011).
49. D. Torrent and J. Sanchez-Dehesa, New J. Phys. **12**, 073034 (2010).

50. D. Torrent and J. Sanchez-Dehesa, Phys. Rev. Lett. **103**, 064301 (2009).
51. Z. Xu, F. Wu, and Z. Guo, Phys. Lett. A: Gener., At. Solid State Phys. **376**, 2256 (2012).
52. J. Redondo, V. Sanchez-Morcillo, and R. Pico, Building Acoustics **18**, 37 (2011).
53. X. F. Li, X. Ni, L. A. Feng, M. H. Lu, C. He, and Y. F. Chen, Phys. Rev. Lett. **106**, 084301 (2011).
54. B. Liang, X. S. Guo, J. Tu, D. Zhang, and J. C. Cheng, Nature Mater. **9**, 989 (2010).
55. B. Liang, B. Yuan, and J. C. Cheng, Phys. Rev. Lett. **103**, 104301 (2009).
56. R. Lucklum and J. Li, Measur. Sci. Technol. **20**, 124014 (2009).
57. S. X. Yang, J. H. Page, Z. Y. Liu, M. L. Cowan, C. T. Chan, and P. Sheng, Phys. Rev. Lett. **88**, 104301 (2002).
58. F. van der Biest, A. Sukhovich, A. Tourin, J. H. Page, B. A. van Tiggelen, Z. Liu, and M. Fink, Europhys. Lett. **71**, 63 (2005).
59. J. O. Vasseur, P. A. Deymier, A. Khelif, P. Lambin, B. Djafari-Rouhani, A. Akjouj, L. Dobrzynski, N. Fettouhi, and J. Zemmouri, Phys. Rev. E: Statist., Nonlinear, Soft Matter Phys. **65**, 056608 (2002).
60. Yu. I. Bobrovnitskii, New J. Phys. **12**, 043049 (2010).
61. M. M. Sigalas and E. N. Economou, J. Sound Vibr. **158**, 377 (1992).
62. J. Mei, Z. Liu, and C. Qiu, J. Phys.: Condens. Matter **17**, 3735 (2005).
63. H. Y. Chen and C. T. Chan, J. Phys. D: Appl. Phys. **43**, 113001 (2010).
64. M. S. Kushwaha, P. Halevi, L. Dobrzynski, and B. Djafari-Rouhani, Phys. Rev. Lett. **71**, 2022 (1993).
65. J. S. Jensen, J. Sound Vibr. **266**, 1053 (2003).
66. X. Zhang, Z. Y. Liu, J. Mei, and Y. Y. Liu, J. Phys.: Condens. Matter **15**, 8207 (2003).
67. D. W. Wright and R. S. C. Cobbold, Smart Mater. Struct. **18**, 015008 (2009).
68. O. Sigmund and J. S. Jensen, Philos. Trans. Roy. Soc. London A: Mathem., Phys. Eng. Sci. **361**, 1001 (2003).
69. Y. W. Yao, Z. L. Hou, and Y. Y. Liu, Phys. Lett. A **362**, 494 (2007).
70. T. Miyashita, Jap. J. Appl. Phys. Part 1: Regular Papers and Short Notes and Review Papers **41**, 3170 (2002).
71. Y. J. Cao, Z. L. Hou, and Y. Y. Liu, Solid State Commun. **132**, 539 (2004).
72. Y. Y. Chen and Z. Ye, Phys. Rev. Lett. **87**, 1843011 (2001).
73. D. Caballero, J. Sanchez-Dehesa, C. Rubio, R. Martinez-Sala, J. V. Sanchez-Perez, F. Meseguer, and J. Llinares, Phys. Rev. E: Statist. Phys., Plasmas, Fluids, and Related Interdisciplinary Topics **60**, R6316 (1999).
74. C. Goffaux and J. P. Vigneron, Phys. Rev. B: Condens. Matter Mater. Phys. **64**, 075118 (2001).
75. Y. Wen-Pei and C. Lien-Wen, Smart Mater. Struct. **17**, 015011 (2008).
76. M. S. Kushwaha, B. Djafari-Rouhani, and L. Dobrzynski, Phys. Lett. A **248**, 252 (1998).
77. M. S. Kushwaha and B. Djafari-Rouhani, J. Appl. Phys. **84**, 4677 (1998).
78. M. S. Kushwaha, B. Djafari-Rouhani, L. Dobrzynski, and J. O. Vasseur, Eur. Phys. J. B **3**, 155 (1998).
79. M. S. Kushwaha and P. Halevi, J. Acoust. Soc. Am. **101**, 619 (1997).
80. V. Romero-Garcia, J. V. Sanchez-Perez, and L. M. Garcia-Raffi, J. Appl. Phys. **108**, 044907 (2010).
81. V. Romero-Garcia, J.V. Sanchez-Perez, S. Castineira-Ibanez, and L.M. Garcia-Raffi, Appl. Phys. Lett. **96**, 124102 (2010).
82. V. Laude, Y. Achaoui, S. Benchabane, and A. Khelif, Phys. Rev. B: Condens. Matter Mater. Phys. **80**, 092301 (2009).
83. V. Romero-Garcia, J. V. Sanchez-Perez, and L. M. Garcia-Raffi, New J. Phys. **12**, 083024 (2010).
84. A. Gupta, K. M. Lim, and C. H. Chew, Appl. Mech. Mater. **152**, 281 (2012).
85. A. Gupta, Numerical modeling and experiments on sound propagation through the sonic crystal and design of radial sonic crystal, *PhD Thesis, Scholarbank NUS,* 2012.
86. A. Gupta, C. Chew, and K. Lim. in *Proc. 4th Int. Conf. on Experimental Mechanics. Singapore, 2009* (Int. Soc. Optics Photonics, 2009).
87. A. G. Webster, Proc. Natl. Acad. Sci. USA **5**, 275 (1919).
88. L. E. Kinsler, A. R. Frey, et al. *Fundamental of Acoustics*, 3rd ed. (Wiley, California, 1982).
89. M. Hirsekorn, P. P. Delsanto, N. K. Batra, and P. Matic, Ultrasonics **42**, 231 (2004).